plaining the peculiar T_1 and T_2 values in Table I and in ref 10. These results can be understood by assuming that the rate of potential fluctuations decreases with increasing polymer M_w. Presumably, this would arise from greater impediments to polymer mobility, impediments that are reflected in an increased solution viscosity and shortened polymer T_2 values as M_w is increased at constant composition.[4] Our observation that $T_1 \sim T_2$ in the low M_w polymer solutions would suggest more rapid potential fluctuations that tend to "symmetrize" the average potential. As shown in an earlier paper,[14] T_1 is relatively insensitive to an asymmetric potential. Since it is only sensitive to the nonsecular high-frequency components of molecular motion, it is insensitive to molecular weight changes unless $M_w < 10^4$.[15]

So far, nothing was said about particular spin relaxation mechanisms. Inspection of Table I shows that the proton T_2 is shortened by an order of magnitude if we compare low and high M_w solutions whereas the corresponding deuteron T_2 is shortened by a factor of 2. Since the deuteron is relaxed by the purely intramolecular quadrupole relaxation, the large effect for the proton T_2 seems to be dominated by an intermolecular mechanism. From our earlier study of PMMA–benzene solutions[10,16] the inter-benzene–polymer contribuion to the proton rate $1/T_1$ is about ⅓ of the total rate in 30% PMMA–benzene solutions. The inter-benzene–polymer contribution to $1/T_2$ should be larger and highly M_w dependent unless our measured T_2 values are influenced by different causes. It should be noted that the concentration gradient in the high M_w solution gives rise to a distribution of susceptibility shifts of the larmor frequencies. However, the resulting contribution to $1/T_2$ is very probably not larger than a few hertz and could only account for part of the short T_2. However, the experimental proton T_2 values differ in an unsystematic fashion for different PMMA samples (see Table I, and Figure 5 of ref 10) that is presently not fully understood.[17]

Acknowledgment. We are grateful to Dr. W. Wunderlich, Röhm GmbH, for supplying the PMMA samples. Support from the Deutsche Forschungsgemeinschaft and the Deutscher Akademischer Austauschdienst is gratefully acknowledged.

References and Notes

(1) B. D. Boss, E. O. Stejskal, and J. D. Ferry, *J. Phys. Chem.*, **71**, 1501 (1967).
(2) R. E. Dehl and C. A. J. Hoeve, *J. Chem. Phys.*, **50**, 3245 (1969).
(3) K.-J. Liu and J. E. Anderson, *J. Macromol. Sci., Rev. Macromol.*, **5**, 1 (1970).
(4) J. E. Anderson, K.-J. Liu, and R. Ullman, *Discuss. Faraday Soc.*, **49**, 257 (1970).
(5) F. W. Wehrli, *Adv. Mol. Relaxation Processes*, **6**, 139 (1974).
(6) B. Boddenberg, R. Haul, and G. Oppermann, *Adv. Mol. Relaxation Processes*, **3**, 61 (1972).
(7) I. Y. Slonim and A. N. Lynbimov, "The NMR of Polymers", Plenum Press, New York, N.Y., 1970.
(8) See, for example, H. Pfeiffer, "NMR, Basic Principles and Progress", Vol. 7, P. Diehl et al., Ed. 1972, p 53.
(9) H. Rockelmann and H. Sillescu, *Z. Phys. Chem. (Frankfurt am Main)*, **92**, 263 (1974).
(10) J. E. Anderson and K.-J. Liu, *J. Chem. Phys.*, **49**, 2850 (1968).
(11) J. Schlegel, Dissertation, Aachen, 1970; R. Kosfeld and K. Goffloo, *Kolloid Z. Z. Polym.*, **247**, 801 (1971).
(12) U. Haeberlen, H. W. Spiess, and D. Schweitzer, *J. Magn. Reson.*, **6**, 39 (1972).
(13) Our model is similar to the "distortable double well" model for dielectric relaxation that was suggested by R. Fuchs and A. von Hippel, *J. Chem. Phys.*, **34**, 2165 (1961). Apart from our consideration of NMR, rather than dielectric relaxation there is one additional difference. We impose the constraint $(k_1/k_2) = (k_3/k_4)$ required by detailed balance; Fuchs and von Hippel do not.
(14) J. E. Anderson, *J. Magn. Reson.*, **11**, 398 (1973).
(15) T. M. Connor, *J. Polym. Sci., Part A-2*, **8**, 191 (1970).
(16) B. Willenberg and H. Sillescu, *Ber. Bunsenges. Phys. Chem.*, **77**, 95 (1973).
(17) NOTE ADDED IN PROOF. After completion of this work, we learned of the NMR study by J. Spevecek and B. Schneider on association of PMMA in solution (private communication and *Makromol. Chem.*, **176**, 3409 (1975), and references quoted therein). About 10–15% of the monomer units in our samples should be part of PMMA aggregates and give rise to decreased benzene T_2 values.

Domain-Boundary Structure of Styrene–Isoprene Block Copolymer Films Cast from Solutions. 2. Quantitative Estimation of the Interfacial Thickness of Lamellar Microphase Systems[1]

Takeji Hashimoto, Akira Todo, Hideyuki Itoi, and Hiromichi Kawai*

Department of Polymer Chemistry, Faculty of Engineering, Kyoto University, Kyoto 606, Japan.
Received July 19, 1976

ABSTRACT: The characteristic parameters of the microdomain structure of alternating lamellae of polystyrene and polyisoprene A–B type block copolymers were estimated by small-angle x-ray scattering. Especially thickness of the domain-boundary interphase was quantitatively estimated by analyzing a systematic deviation of the scattering curves at large angle tail from the Porod's law. The experimental thicknesses of the domain and domain-boundary interphase were qualitatively in agreement with those predicted by current theories of statistical mechanics of the microdomain formation by Meier and Helfand. However, problems are still open to be clarified in quantitative comparisons of the experimentally observed thin interphase ranging from 19 to 22 Å with the thickness predicted by the current theories which assume relatively thick interphase or small value of the interaction parameter χ.

In the previous paper of this series,[2a] which will be called hereafter part 1, the microdomain structures of polystyrene–polyisoprene A–B type block copolymer films cast from toluene solutions were investigated by means of electron microscopic and small-angle x-ray scattering (SAXS) methods. The copolymers studied were those having chemical compositions giving rise to the domain structure of alternating lamellae of A and B components. It was demonstrated that the lamellae are highly oriented with their normals perpendicular to the bulk film surface (see Figures 1 to 3) and proposed that the meridional SAXS intensity distribution, i.e., the intensity distribution parallel to the lamellar normal, may be analyzed in terms of a scattering theory based upon one-dimensional paracrystal model of Blundell.[2b]

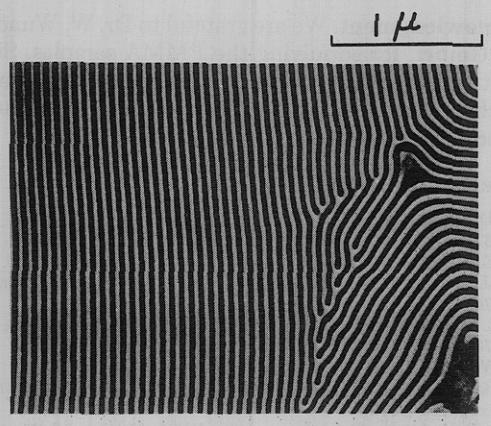

Figure 1. Typical electron micrograph of ultrathin section of the specimens stained by osmium tetroxide and cut normal to the specimen surfaces.

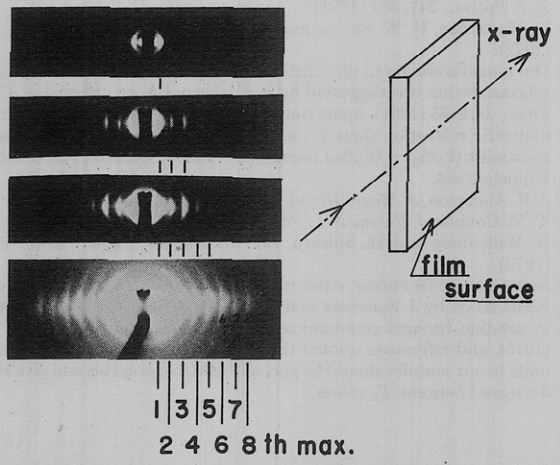

Figure 2. Small-angle x-ray scattering patterns of the specimens taken with Huxley–Holmes camera. The patterns were taken with different exposures and with the incident x-ray beam parallel to the specimen surfaces as shown in the figure.

The analyses yielded quantitative evaluations of structural parameters of the domain systems;[2a] i.e., (a) the mean periodic distance $\bar{x}$ of lamellae, (b) the paracrystalline disorder of the periodic distance σ_X, and (c) the volume fraction of the respective domains. Some other structural parameters were also estimated qualitatively. These are the size of the grain parallel and perpendicular to the lamellar normals $\bar{N}$ and R, and the thickness of the domain boundary region t. The parameter t is related to a degree of partial mixing of block chains at the boundary.

In this paper, the most attention is focussed on a quantitative estimation of the parameter t by analyzing the tail of the SAXS intensity distribution at large scattering angles. The estimation of the parameter t was performed for a particular copolymer designated as SI-L in part 1 for which the one-dimensional analyses of x-ray scattering intensity distribution were shown to be legitimate with a high accuracy. The estimated value of t will be compared with those expected from current statistical thermodynamic theories of the interface between two phases in block copolymers.[3-10]

Test Specimens

The specimens, styrene–isoprene A–B type block copolymers, were prepared by anionic polymerization according to the method described in the previous paper.[11] The weight

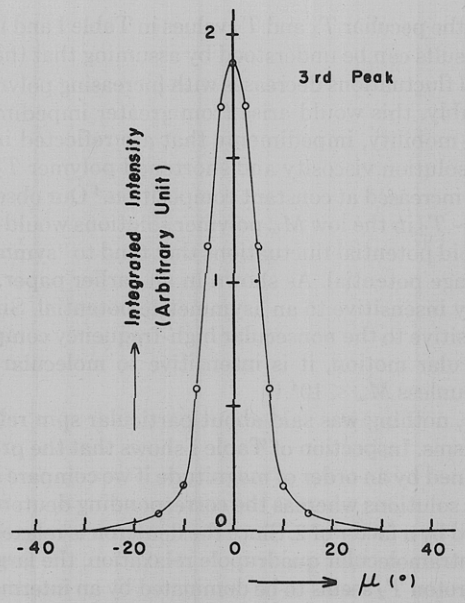

Figure 3. Microdensitometer scanning of azimuthal angle dependences of the integrated scattered intensity under the third scattering maximum shown in Figure 2. The meridional direction corresponds to $\mu = 0°$.

percent of polystyrene is 59 and the total number-average molecular weight is 1.05×10^5. The copolymers were cast into thin films of about 100 μm thickness by pouring 5% toluene solution onto a glass plate floating on mercury and by evaporating the solvent very gradually at 30 °C for a few days. The film specimens thus formed were further dried in a vacuum line (10^{-6} mm) for several days until the specimens were at constant weight. The as-cast films thus prepared were further annealed at a temperature above the glass transition temperature of polystyrene block, 126 °C, for 24 h under a vacuum of 10^{-6} mm in a case when effects of annealing on the domain structure are to be investigated.

Results

Figure 1 shows a typical electron micrograph of an ultrathin section of the specimens stained by osmium tetroxide. The dark and bright phases corresponding to the polyisoprene and polystyrene domains are shown to be arranged regularly and alternatively. Figure 2 shows a typical small-angle x-ray scattering pattern taken with a x-ray beam parallel to the film surfaces. The pattern was taken with a point focussing camera (No. 1555, Rigaku Denki) composed of a bent mirror as a horizontal reflector and a bent quartz monochrometer as a vertical reflector. The camera system is equivalent to a Huxley-Holmes camera. A high brilliancy rotating anode x-ray generator (Rigaku Denki) was used as a microfocussed x-ray source. The focal size is 0.1×1.0 mm^2 and 0.1×0.1 mm^2 in projection. The pattern was taken with Cu Kα radiation and with a power of 40 kV and 30 mA for various exposure times. The camera length was set at 280 mm. The pattern corresponding to Figure 2a of ref 2a was taken with a conventional low-angle x-ray camera (No. 2202, Rigaku Denki).

The SAXS pattern shows that the lamellar microdomains are highly oriented with their boundaries parallel to the surfaces of the film specimens, although there exists a slight orientation distribution of the lamellae. Figure 3 shows dependence of integrated SAXS intensities under the third scattering maximum shown in Figure 4 with azimuthal angles μ as measured by microdensitometer scanning of the patterns shown in Figure 2, where $\mu = 0°$ corresponds to the integrated intensity on the meridian. The result indicates that the lam-

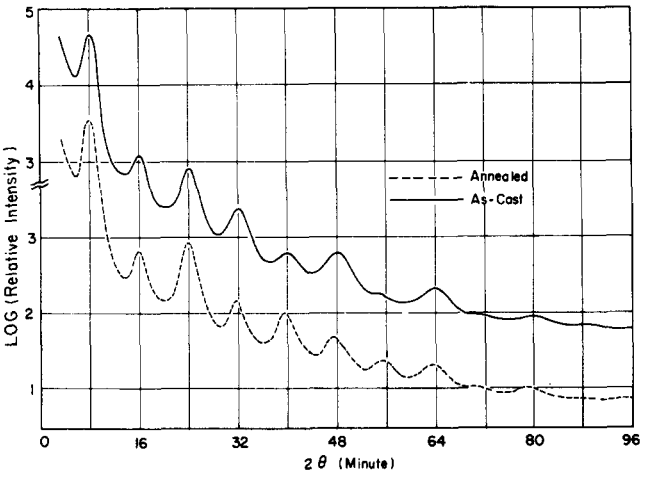

Figure 4. The meridional small-angle x-ray scattering intensity distributions for the as-cast and annealed specimens.

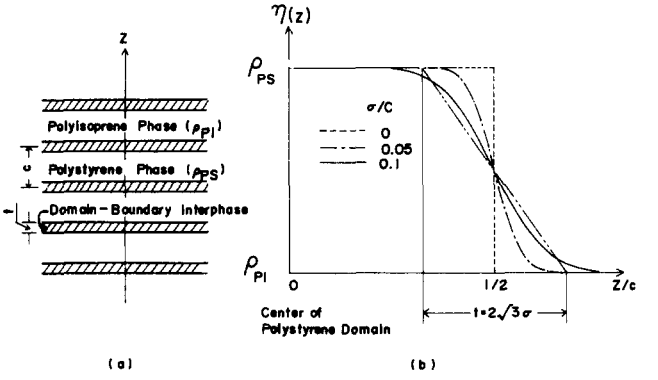

Figure 5. The model of alternating lamellar microdomain structure (a) and the assumed electron density profiles (b).

ellae can be assumed to orient almost perfectly with the z axis normal to the film surfaces (see Figure 5) with a good approximation.

Figure 4 shows the SAXS intensity distributions along the meridional direction, i.e., direction normal to the film surfaces for the as-cast and annealed specimens. The intensity distributions were measured with a scintillation counter and a rotating anode x-ray generator (Rotaflex RU-100FL, Rigaku Denki) with a power of 50 kV and 100 mA and with line focussing under a similar collimating system as in the previous paper;[2a] i.e., the first, the second, and the third slits and the specimen, the counter, and scattering slits, were placed at 128, 378, 418, 443, 703, and 743 mm from the focal spot, respectively, and the sizes of the focal spot and the first, second, counter, and scattering slits are 1.5 × 5, 0.1 × 10, 0.1 × 10, 0.1 × 15, and 0.5 × 15 mm^2, respectively. The intensity was measured with Ni-filtered Cu Kα radiation and pulse-height analyzer and with a step scanning device with a step interval of 0.6 min, each at a fixed time of 200 s. The film surface is set parallel to the line source of the x-ray beam, so that the line becomes parallel to the boundaries between the polystyrene and polyisoprene microdomains. In this arrangement the scattered intensity distribution should not be affected much by the effect of slit-height smearing[13] because of the almost perfect orientation of lamellar microdomains. Consequently, the correction for the effect was not performed in the following analyses.

As seen in Figure 4, the scattering curves for both as-cast and annealed films contain, at least, ten resolvable scattering maxima, each of which is associated with a higher order diffraction maximum of a single spacing of 660 Å (corresponding to ca. 8 min in the 2θ scattering angle) and 670 Å for the as-cast and annealed specimens, respectively. The number of scattering maxima ranging, at least, up to 10 indicates that the standard deviation of the fluctuation in repeat distance must be less than 4% of the average repeat distance $\overline{X}$ according to Blundell analysis.[2] In the previous work, however, the intensity distribution was measured with a counting-rate meter so that the higher order scattering maxima greater than the ninth order were not clearly resolved.

In the previous paper[2a] the effect of annealing the as-cast specimens below and above the glass transition temperature of polystyrene block chains was investigated. The results indicated that the annealing at temperatures above the glass transition thickens the interlamellar spacing as a consequence of an expansion of each phase. Upon annealing, the spacing increased from 590 to 660 Å, the latter value of which agrees with those observed in this work both for the as-cast and annealed specimens.

In this work, the lamellar expansion was not essentially observed and the spacing of the as-cast films was almost identical with that of the annealed films. We feel, at present, that the spacings 660 and 670 Å of the as-cast and annealed specimens in this work are closer to that expected in the equilibrium state than the spacing 590 Å observed previously for the as-cast specimens. The variation of the spacing in as-cast specimens may be due to the nonequilibrium effect in the process of solvent evaporation as discussed in the previous paper. It should be pointed out, however, that the spacing and the volume fraction of polystyrene domain tend to expand and decrease, respectively, slightly upon annealing above the glass transition temperature, the tendencies of which are similar to those in the previous work.

Hereafter, we analyze the SAXS intensity distribution at large angle tails for a quantitative analyses of the domain-boundary structure where the interference function approaches unity and the scattering solely depends upon each domain structure.

Theoretical Background on Estimating the Domain-Boundary Thickness of Lamellar Microdomain Systems

The system to be considered here is the one which has one-dimensional electron density fluctuation along a direction normal to the lamellar interfaces as shown in Figure 5. The density variation $\eta(z)$ along the z axis is periodic due to a periodic and alternating arrangement of polystyrene and polyisoprene lamellae. The variation generally deviates from the variation $g(z)$ of an ideal two-phase system in which the density variation occurs discontinuously from ρ_{PS} to ρ_{PI}, ρ_{PS} and ρ_{PI} being the electron densities of polystyrene and polyisoprene domains, respectively.

The function $\eta(z)$ may have, in general, a variation characteristic for a pseudo-two-phase system in which the density continuously varies from ρ_{PS} to ρ_{PI} or vice versa over a finite transition region because of partial mixing of the incompatible block chains at the domain interfaces. Let $h(z)$ be a smoothing function related to the thickness of the domain boundary region, then the function $\eta(z)$ for the pseudo-two-phase system is given by the one-dimensional convolution product of the functions $g(z)$ and $h(z)$;

$$\eta(z) = g(z)*h(z) = \int_{-\infty}^{\infty} g(u)h(z-u)\,du \qquad (1)$$

The structure amplitude of the system $F(s)$ is given by Fourier transform of the function $\eta(z)$;

$$F(s) = \mathfrak{F}\{\eta(z)\} \qquad (2)$$

$$\mathcal{F}\{\eta(z)\} = \int_{-\infty}^{\infty} \eta(z) \exp(2\pi isz)\, dz \tag{3}$$

where

$$s = 2 \sin \theta/\lambda \tag{4}$$

where λ is the wavelength of the x ray and 2θ is the scattering angle. Here we consider only scattering parallel to the z direction, i.e., meridional scattering. From eq 1 and 2, it follows that

$$F(s) = \mathcal{F}\{g(z)\}\mathcal{F}\{h(z)\} \tag{5}$$

Thus the scattering intensity $I(s)$ of the system is given by

$$I(s) = I_e|F(s)|^2 = I_g(s)I_h(s) \tag{6}$$

where

$$I_g(s) = |\mathcal{F}\{g(z)\}|^2 \tag{7}$$

$$I_h(s) = |\mathcal{F}\{h(z)\}|^2 \tag{8}$$

and I_e is the Thomson scattering intensity from an electron.

The function $I_g(s)$ corresponds to the scattering intensity from the ideal two-phase system, which is given for isotropic systems according to Porod's law[14] or to the calculation of Debye–Anderson–Brumberger[15] as

$$I_g(s) = C_1 s^{-4} \tag{9}$$

where C_1 is a constant related to $(\rho_{PS} - \rho_{PI})^2$ and the total area of the interface S,

$$C_1 = I_e(\rho_{PS} - \rho_{PI})^2 S/(2\pi)^3 \tag{10}$$

However, if the lamellar domains are perfectly oriented in a manner as described above, one should modify eq 9, as indicated in the Appendix, as follows:

$$I_g(s) = C_2 s^{-2} \tag{11}$$

If the smoothing function $h(z)$ is given by a step function, as given by Vonk,[16]

$$h(z) = \begin{cases} 1/t & \text{for } 0 \le z \le t \\ 0 & \text{for } z > t \end{cases} \tag{12}$$

then the electron density variation $\eta(z)$ is given by a trapezium profiles, as shown in Figure 5b. In this case, $I_h(s)$ is readily obtained from eq 8 and 12,[16]

$$I_h(s) = \sin^2(\pi st)/(\pi st)^2 = 1 - (\pi st)^2/3 + \mathcal{O}[(\pi st)^4] \tag{13}$$

On the other hand, if the function $h(z)$ is given by a Gaussian function,

$$h(z) = (2\pi\sigma^2)^{-1/2} \exp(-z^2/2\sigma^2) \tag{14}$$

with a standard deviation σ, the electron density varies sigmoidally from one phase to another, as shown in Figure 5b. From eq 8 and 14, it follows that

$$I_h(s) = \exp(-4\pi^2\sigma^2 s^2) = 1 - 4\pi^2\sigma^2 s^2 + \mathcal{O}[(\pi\sigma s)^4] \tag{15}$$

Therefore, the observed meridional SAXS intensity distribution $I(s)$ for the pseudo-two-phase system is given by

$$I(s) = (\text{constant}) s^{-2}[1 - (\pi^2 t^2/3)s^2 + \mathcal{O}[(\pi st)^4] \tag{16a}$$

or

$$I(s) = (\text{constant}) s^{-2}[1 - (4\pi^2\sigma^2)s^2 + \mathcal{O}[(\pi\sigma s)^4] \tag{16b}$$

If t or σ is small compared with the size of the lamellar domain, the higher order terms in the last terms of eq 16a and 16b are negligible.[24] Consequently, a plot of $I(s)$ against s^{-2} gives a straight line, the slope and intercept of the line at $s^{-2} = 0$ giving rise to a parameter t or σ which characterizes the domain-boundary thickness. It should be noted that the scattered intensity distribution at the large angle tail for a system with sigmoidally varying electron density profile at the transition region is identical with that for a system with linearly varying density profile at the transition region, provided that a following relationship is applicable between t and σ,

$$t = 2(3)^{1/2}\sigma \tag{16c}$$

Experimental Analyses of the Interfacial Thickness t

Figure 5b shows assumed electron density profiles at the interphase, i.e., the interfacial region. A series of sigmoidal profiles is given by varying σ in the Gaussian smoothing function, eq 14, and a straight line profile is given by using eq 12. It is obvious that the density transition at the interphase becomes diffuse with increasing σ and t.

Figure 6 shows the SAXS intensity distributions of the specimens, at even larger scattering angles than those in Figure 4. It is seen that the scattered intensity increases with increasing the scattering angle due to an increasing contribution of amorphous scattering of polystyrene block.[25] We subtracted the background scattering I_b arising from the amorphous order and thermal density fluctuation from the total scattered intensity. This is purely an empirical procedure. The background scattering was assumed to be given by a straight line as shown in the figure. It should be noted that one can choose a curved background scattering as in Vonk's work.[16] However, the manner of subtracting the background scattering did not much affect the final value of σ or t (the difference was less than 10%).

Now from eq 16a or 16b, it follows that for small values of t or σ,

$$I(s) = (\text{constant})[s^{-2} - (\pi^2 t^2/3)] \tag{16d}$$

or

$$I(s) = (\text{constant})[s^{-2} - 4\pi^2\sigma^2] \tag{16e}$$

Figure 7 shows the plots of $I(s)$ against $s^{-2} \times 10^{-3}$ for the as-cast and annealed specimens. It is obvious from the figure that there exists the domain-boundary region of a finite thickness. The thickness t estimated on the basis of eq 16d turned out to be 19 and 22 Å for the annealed and as-cast films, respectively. The overall volume fraction of the domain-boundary region is 5.7 and 6.7% for the annealed and as-cast films, respectively. Therefore, the annealing tends to decrease slightly the volume fraction of the mixed region.

Comparison with the Theories of the Microphase Separation

Meier has developed a statistical thermodynamic theory of the microphase separation,[3-5] and Meier–Inoue have extended the theory to the system composed of the mixture of block copolymer with homopolymers.[6] In their theory of the interface in block copolymers[5,6] it was assumed that the block copolymer is a single A–B type with chains of both blocks having equal bulk densities, equal molecular weights, equal unperturbed statistical segment length, and following the random-flight statistics.[26] Figure 8 shows the assumed structure of the interfacial region (interphase) in which the relative densities of segments of the A and B block chains smoothly change from zero to unity in the interphase of thickness λ_M. Special functions were assumed for the volume fractions of A and B segments in the interphase, respectively, as follows;[5,6]

$$\phi_A(z) = \sin^2(\pi z/2\lambda_M)$$

$$\phi_B(z) = \cos^2(\pi z/2\lambda_M) \tag{17}$$

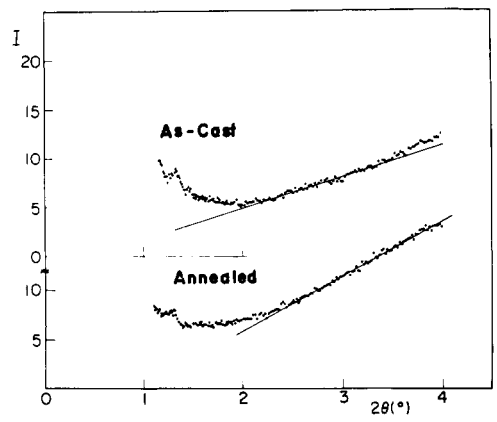

Figure 6. The small-angle x-ray scattering intensity distribution of the specimens at larger angles than those in Figure 4.

Free energy of the system was calculated by taking into account (i) the interfacial contact energy ΔE based upon Cahn-Hilliard formulation for nonuniform system

$$\Delta E = \frac{\chi_{AB}kT}{\bar{v}_A}\int [\phi_A\phi_B + (1/6)t_D^2(d\phi_A/dz)^2]\,dv \quad (18)$$

where ΔE is the interfacial contact energy per unit area of the interphase relative to the pure components, χ_{AB} is Flory–Huggins interaction parameter between A and B components, $\bar{v}_i$ is the molecular volume of the ith component, and t_D is Debye's interaction range parameter being assumed as about 8 Å; (ii) the placement entropy ΔS_p, an entropy loss involved in restricting the A–B junction point within the interphase

$$\Delta S_p = Nkln(A\lambda_M/V) \quad (19)$$

where A is the cross-sectional area of the interface, and N is the number of block copolymers within the total volume V of the system; and (iii) the entropy of constrain volume ΔS_v, additional entropy loss encountered by restricting A and B segments in their respective domains. This entropy was derived by solving a diffusion equation on a probability function $P_n(z,z')$ under a proper boundary (absorptive boundary) and initial conditions and by obtaining the probability density of $P(T_A,T_B,\lambda_M)$ as follows;

$$\partial P_n(z,z')/\partial n = (l^2/6)\nabla^2 P_n(z,z') \quad (20)$$

where $P_n(z,z')$ is a probability of the chain having n statistical segments of length l with one end at z and the other end at z', and $P(T_A,T_B,\lambda_M)$ is the probability that the junction point of the A–B block is in the interphase of thickness λ_M and all segments of A and B blocks are within their proper domains of thickness T_A and T_B. The constrained volume entropy is then given by

$$\Delta S_v = kNln[P(T_A,T_B,\lambda_M)] \quad (21)$$

The free energy of the microdomain formation of the block copolymers has been finally given by[6]

$$\frac{\Delta G_d}{NkT} = \frac{\chi_{AB}\lambda_M}{4T_A} - ln(\lambda_M/T_A)^3 - 2ln\sum_{\substack{m=1\\(odd)}}^{\infty}(-1)^{(m+3)/2}m\exp(-\pi^2m^2/12\alpha^2) + (\text{constant}) \quad (22)$$

where the last term of the right-hand side of eq 22, a constant, is a term independent of λ_M and chain expansion coefficient α ($=\alpha_A = \alpha_B$). Equation 22 is a limiting case of the free energy of microdomain formation of a system composed of a mixture of block copolymer with corresponding homopolymers in

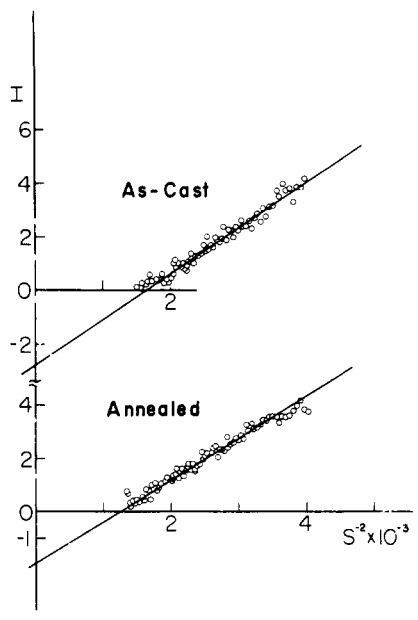

Figure 7. The plots of $I(s)$ against $s^{-2} \times 10^{-3}$ for the as-cast and annealed specimens to obtain the thickness t of the interphase.

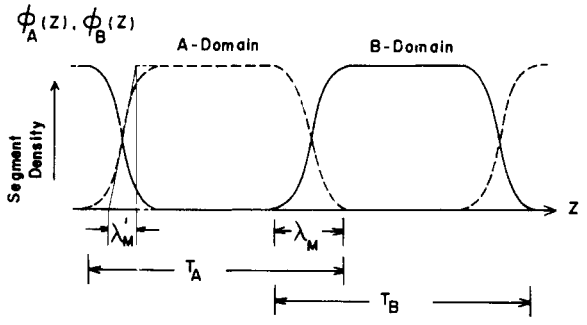

Figure 8. The assumed structure of the interphase in the statistical mechanical calculations.

which each fraction of homopolymer added is extrapolated to zero. Equation 22 is based on the assumption that the interphase is thick enough compared with t_D so that the second term of eq 18 is neglected. In the case of t_D being not negligible, the first term of the right-hand side of eq 22 should be replaced with[5]

$$\frac{A\chi_{AB}}{N\bar{v}_A}\int_0^{\lambda_M}[\phi_A\phi_B + (1/6)t_D^2\,(d\phi_A/dz)^2]\,dz \cong \frac{\chi_{AB}(6\lambda_M^2 + \pi^2t_D^2)}{24T_A\lambda_M} \quad (23)$$

It should be noted that the segment density distribution within a domain can be calculated on the basis of P_n as a function of the ratio of domain size T_A to chain dimension $(n_Al^2)^{1/2}$. The requirement that the segment density within the domains must be uniform yielded the following relationship;[4]

$$T_A = T_B = T = 1.4(nl^2)^{1/2} = 1.4\alpha(nl^2)_0^{1/2} = 1.4\alpha KM^{1/2} \quad (24)$$

where K is an experimental constant relating the unperturbed chain dimension $(nl^2)_0^{1/2}$ to molecular weight M.

Equilibrium values of λ_M and α are obtained by minimizing the free energy,

$$\partial(\Delta G_d/NkT)/\partial\alpha = 0$$
$$\partial(\Delta G_d/NkT)/\partial\lambda_M = 0 \quad (25)$$

Equations 22 and 25 give

$$\alpha = \alpha_A = \alpha_B = 2^{1/2} \quad (26)$$

$$\lambda_M = (6T_A/\chi_{AB}) + [(6T_A/\chi_{AB})^2 + (1/6)\pi^2 t_D^2]^{1/2} \quad (27)$$

In order to compare the interfacial thickness λ_M with that calculated by Helfand[9,10] and with that estimated from small-angle x-ray scattering experiment (t), the thickness λ_M should be transformed to the thickness λ_M' as shown in Figure 8. Obviously, the following relationship is obtained;

$$\lambda_M' = 0.6366\lambda_M \quad (28)$$

A similar but more elaborate theory has been developed by Helfand.[7-10] He has started with a modified diffusion equation with the term U_A (or U_B) associated with the work needed to transfer a segment of A (or B) from pure A (or B) to a region with B (or A) content,

$$\frac{\partial Q_A(z,n;z')}{\partial n} = \left[(b_A^2/6)\nabla^2 - \frac{U_A(z)}{kT} \right] Q_A(z,n;z') \quad (29)$$

where Q_A corresponds to P_n in Meier's equation, and n and b_A in eq 29 are number and length of the Kuhn statistical segment, respectively. In his mean field approximation, the field U_A is generated by the other molecules and by other parts of itself and is composed of two terms; (i) the term related to interaction with B and thus having a form proportional to χ and the local volume fraction of B, and (ii) the term arising from the cohesive forces which tend to maintain the overall density to be uniform as ρ_0 (number of segments per unit volume) and thus having a form of

$$kT\zeta[\rho_A(r) + \rho_B(r) - \rho_0]/\rho_0$$

$$\zeta = (\rho_0 kT\kappa)^{-1}$$

where κ is the compressibility. The quantity χ is the interaction parameter defined by

$$\chi = (\delta_A - \delta_B)^2/\rho_0 kT \quad (30a)$$

where δ_A and δ_B are solubility parameters of the respective block chains. The χ parameter defined by Helfand[12] is related to χ_{AB} defined by Meier as

$$\chi_{AB} = \chi Z_A \quad (30b)$$

where Z_A ($=Z_B = Z$) is the degree of polymerization of A and B block chains.

The modified diffusion equation is solved for a symmetric AB block copolymer, yielding the density distribution, $\rho_A(Z)$ and $\rho_B(Z)$, and the free energy.

More recently Helfand and Wasserman[19,20] have solved the equations in an approximate fashion, appropriate when the interphase is narrow compared with the width of the domain. They conclude that the density across the interphase approaches that between the corresponding homopolymers, as described by Helfand and Tagami[10] for a symmetric pair of polymers, and by Helfand and Sapse[18] for an unsymmetric pair. An explicit formula for the domain size has been obtained, which predicts a domain repeat distance of 550 Å for the block copolymer studied in this report.

Helfand's full solution and narrow interphase approximation have been contrasted[20] for a symmetric block copolymer and for the explicit χZ values of 37 and 10, where Z is the degree of polymerization of each block as defined above. For small χZ, interpenetration of A and B is quite extensive. For $\chi Z = 10$ significant excess interpenetration was shown to occur for the block copolymers compared with the homopolymer blends. However, with increasing value of χZ, up to 37, the interphases of block copolymers and homopolymer blends were shown to be very similar. The block copolymer studied in this paper is diblock polystyrene–polyisoprene having molecular weight of 6.1×10^4 and 4.4×10^4, respectively, corresponding to an average[9] Z of 615. If the χ value of polystyrene–polyisoprene interaction is 0.142, as employed by Helfand,[9] then $\chi Z = 87$, so the interphase of the block copolymer should be quite close to that between semiinfinite phases of homopolymer blends. Helfand and Tagami[10] have shown that for a small value of χ a characteristic interfacial width λ_{HT} of the homopolymer blend is given by

$$\lambda_{ht}, 2b/(6\chi)^{1/2} \quad (31)$$

where b is Kuhn's statistical segment length. The value of b was chosen to be 6.6 Å by Helfand[9] for the SI block copolymer, so as to obtain correspondence with formulas appropriate to unsymmetric interfaces.[18] It should be noted that the thickness λ_{HT} corresponds to the thickness λ_M'.

From eq 31, λ_{HT} turns out to be 14.3 Å for $\chi = 0.142$ and $b = 6.6$ Å, for which the value of χ was again adopted from a paper by Helfand.[9] The experimental value of the interphase thickness (19 Å to 22 Å) is a little higher than the λ_{HT} value, which is reasonable since λ_{HT} in eq 31 should give the lower limit expected for infinitely large molecular weights of the copolymers.

Now let us compare our results with those predicted by Meier. From eq 24 and 26, we can estimate the equilibrium periodic distance $2T$ of the alternating domain structure, i.e.,

$$2T = 4KM^{1/2} \quad (32)$$

Assuming $K = 7.5 \times 10^{-1}$ Å, as Meier did,[4,5] then

$$2T = 4 \times 7.5 \times 10^{-1} \times (10.5 \times 10^4/2)^{1/2} = 687 \text{ Å}$$

The value of 687 Å is in good agreement with the observed periodic distances of 660 and 670 Å for the as-cast and annealed specimens. From eq 27, we can estimate the thickness of the interphase predicted from Meier's theory. It should be noted that χ_{AB} in eq 22, 23, and 27 is related to χ defined by Helfand and Tagami as in eq 30b. In our block copolymer, $Z = 615$, and assuming χ to be 0.142 and t_D to be 0, then λ_M and λ_M' turned out to be 47.2 and 30.1 Å, respectively. If t_D is 8 Å, as Meier assumed, then λ_M and λ_M' must be 49.3 and 31.4 Å, respectively. The estimated values of λ_M' are again in fairly good agreement with the observed values, though the estimated values are, in contrast, a little higher than the observed values of 22 and 19 Å for the as-cast and annealed specimens, respectively. Table I summarizes the experimental and theoretical results.

It should be noted that Meier and Helfand assumed that the interphase is thin enough so that there are domains of essentially pure A and B components but, at the same time, thick enough so that the Debye interaction range parameter t_D is small compared with the thickness of the interphase (see eq 18 by Meier) or the χ parameter is relatively small to give eq 31 by Helfand and Tagami. The experimentally observed values ranging from 19 to 22 Å are fairly small, i.e., only ca. 2.5 times the Debye interaction range parameter[27] or only ca. 3 times the statistical segment length. Therefore, it may be open to criticism to compare in a quantitative manner such thin interphase with the interphase predicted from the current theories.

Figure 9 shows a proposed microdomain structure of the annealed block copolymer films where relative electron density profile along the z direction is shown in Å scale. The phases with high and low densities correspond to those of polystyrene and polyisoprene domains, respectively. The volume fraction of polystyrene domain, 0.545, was obtained from the previous analyses.[2a] Figure 9a shows the density variation at the interphase calculated from eq 1, 14, and 16c

Table I
Comparison of Theoretical and Experimental Results[e]

Periodic distance, Å			Characteristic interfacial thickness, Å		
Obsd	Meier[a]	Helfand[b]	Obsd t	$\lambda_M{}'$[c]	λ_{HT}[d]
670	687	550	19	31.4	14.3
(660)			(22)		

[a] Calculated based upon eq 32. [b] Reference 19. [c] Calculated from eq 27 by assuming t_D = 8 Å and χ = 0.142 (Meier). [d] Calculated from eq 31 by assuming b = 6.6 Å and χ = 0.142 (Helfand and Tagami). [e] The values in parentheses are the observed ones for as-cast specimen.

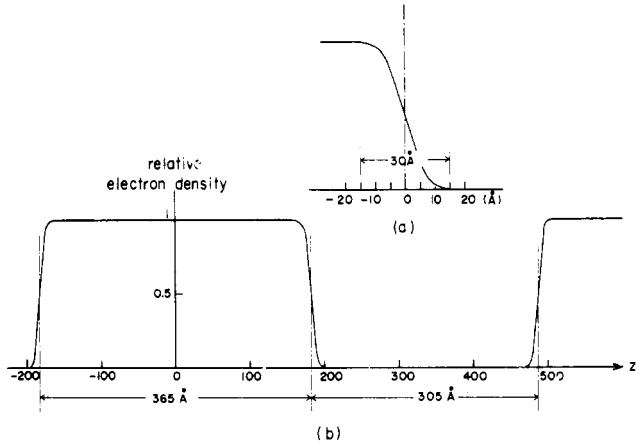

Figure 9. The proposed microdomain structure of annealed specimens where relative electron density profile along the z direction is shown in the Å scale.

with t = 19 Å. The thickness of the interphase corresponding to λ_M in Figure 8 is 30 Å as shown in the figure. Figure 9b shows the relative electron density variation across the polystyrene and polyisoprene domains.

Acknowledgment. The authors acknowledge Drs. D. J. Meier, Midland Macromolecular Institute, Midland Mich., E. Helfand, Bell Laboratories, Murray Hill, N.J., and T. Inoue, the Research Center, the Japan Synthetic Rubber Co., Ltd., Kawasaki, Japan, for their valuable discussions and comments and Dr. H. Kurata, the Rigaku Denki Ltd., Haijima, Tokyo, Japan, for kindly taking the small-angle x-ray scattering patterns in Figure 2. This work is supported in part by a scientific research grant through the Mitsui Petrochemical Industries, Ltd., Tokyo, Japan, the Japan Synthetic Rubber Co., Ltd., Tokyo, Japan, and the Bridge Stone Tire Co., Ltd., Tokyo, Japan.

Appendix. The s^{-2} Dependence of Low-Angle X-Ray Scattering Intensity Distribution at Large Scattering Angle Tail for the Ideal Two-Phase Structure Composed of Completely Oriented Lamellar Microdomains

In general scattered intensity for any system is given by

$$I_s = I_e \langle \eta^2 \rangle V \int \gamma(\mathbf{r}) \exp[i(\mathbf{h} \cdot \mathbf{r})] \, d\mathbf{r} \qquad (A1)$$

where mean square electron density fluctuation $\langle \eta^2 \rangle$ is given for the ideal two-phase system by

$$\langle \eta^2 \rangle = (\rho_1 - \rho_2)^2 \phi_1 \phi_2 \qquad (A2)$$

where ρ_i and ϕ_i are electron density and volume fraction of ith phase. The function $\gamma(r)$ is the correlation function of the density fluctuation which is a function of $|\mathbf{r}|$ only for an isotropic system. The variable $\mathbf{h}$ is a scattering vector defined as $(2\pi/\lambda)(\mathbf{s}_0 - \mathbf{s}')$ where the unit vectors $\mathbf{s}_0$ and $\mathbf{s}'$ correspond to the propagation directions of the incident and scattered rays, respectively, and the magnitude of it is given by $h = (4\pi/\lambda) \sin\theta$ where 2θ is the scattering angle. V is irradiated volume by x ray.

For an isotropic and ideal two-phase system, it follows from eq A-1 and A-2 that

$$I_s = I_e V (\rho_1 - \rho_2)^2 \phi_1 \phi_2 \int_0^\infty \gamma(r) (\sin hr/hr) 4\pi r^2 \, dr \qquad (A3)$$

The function $\gamma(r)$ at small r is given by Debye–Anderson–Brumberger[15] as

$$\gamma(r) = 1 - (S_{sp}/4\phi_1\phi_2)r + \ldots \qquad (A4)$$

where S_{sp} is specific surface of the system which is defined as a ratio of total area of the interfaces S of the two phases to the total volume of specimen, i.e., the irradiated volume of specimen V. From eqs A-3 and A-4, it follows that

$$\lim_{h \to \infty} I_s = I_e (\rho_1 - \rho_2)^2 2\pi S h^{-4} \qquad (A5)$$

Thus, at large scattering angle, so-called Porod's law of h^{-4} or s^{-4} is valid, where s is defined by $2 \sin\theta/\lambda$.

For an oriented system, one must start with eq A1 instead of eq A3. For the sake of simplicity, let us first consider an isolated lamellar domain with no transition zone (domain boundary zone) perfectly oriented with its normal along the z axis. The meridional scattered intensity of the system, i.e., the intensity scattered along the z axis, $I(h_3)$ is then given by

$$I_s(h_3) = I_e V_p (\rho_1 - \rho_2)^2 \int\int\int_{-\infty}^{\infty} \gamma_0(x,y,z) \times \exp(ih_3 z) \, dx \, dy \, dz \qquad (A6)$$

where h_3 is a component of scattering vector $\mathbf{h}$ along the z axis, and ρ_1 and ρ_2 are the electron densities of the lamella and its surrounding medium, respectively. V_p is the volume of the lamella. The function $\gamma_0(x,y,z)$ is the correlation function of the lamellar domain with constant density ρ_1 within it. From eq A6, it follows that

$$I_s(h_3) = I_e V_p (\rho_1 - \rho_2)^2 \int_{-\infty}^{\infty} \gamma_1(z) \exp(ih_3 z) \, dz \qquad (A7)$$

where

$$\gamma_1(z) = \int_{-\infty}^{\infty} \gamma_0(x,y,z) \, dx \, dy$$

The one-dimensional correlation function $\gamma_1(z)$ is given by

$$\gamma_1(z) = \begin{cases} S_p(1 - |z|/c)/2 & \text{for } |z| \le c \\ 0 & \text{for } |z| > c \end{cases} \qquad (A8)$$

where c is the dimension of the lamella along the z axis, and the total surface area normal to the scattering vector S_p can be defined by

$$S_p = (2/c) V_p \qquad (A9)$$

If the shape of the domain is more complex than the lamella,

then there should be higher terms of z in the function $\gamma_1(z)$. Now from eq A7 through A9, it follows that at large scattering angles

$$\lim_{h_3 \to \infty} I_s(h_3) = I_e(\rho_1 - \rho_2)^2 S_p^2 h_3^{-2} \quad \text{(A10)}$$

For the two-phase system composed of N perfectly oriented lamellae, S_p in eq A10 should be replaced with S given by

$$S = NS_p \quad \text{(A11)}$$

where S is the total surface area of the lamellar microphase system normal to the z axis. Therefore, the scattered intensity at large angle tail for the completely oriented ideal two-phase structure is given by

$$\lim_{h_3 \to \infty} I_s(h_3) = I_e(\rho_1 - \rho_2)^2 S^2 h_3^{-2} \quad \text{(A12)}$$

Equation A12 corresponds to eq A5 for the isotropic and ideal two-phase structure. The reduced scattering angle h_3 in eq A12 also corresponds to the variable $2\pi s$ in the text, so that eq A12 can be rewritten by

$$\lim_{s \to \infty} I_s = [I_e(\rho_1 - \rho_2)^2 S^2 / 4\pi^2] s^{-2} \quad \text{(A13)}$$

References and Notes

(1) Presented partly at the 24th Symposium on Polymer Chemistry, Japan, Osaka University, Nov. 6, 1975.
(2)(a) T. Hashimoto, K. Nagatoshi, A. Todo, H. Hasegawa, and H. Kawai, *Macromolecules*, **7**, 364 (1974); (b) D. J. Blundell, *Acta Crystallogr., Ser. A*, **26**, 472, 476 (1970).
(3) D. J. Meier, *J. Polym. Sci., Part C.*, **26**, 81 (1969).
(4) D. J. Meier, *Polym. Prepr., Am. Chem. Soc., Div. Polym. Chem.*, **11**, 400 (1970).
(5) D. J. Meier, *Polym. Prepr., Am. Chem. Soc., Div. Polym. Chem.*, **15**, 171 (1974).
(6) T. Inoue and D. J. Meier, paper presented at the 24th Symposium on Polymer Chemistry, Japan, Osaka University, Nov. 6, 1975.
(7) E. Helfand, *Polym. Prepr., Am. Chem. Soc., Div. Polym. Chem.*, **14**, 970 (1973).
(8) E. Helfand, "Recent Advance in Blends, Grafts, and Blocks", L. H. Sperling, Ed., Plenum Press, New York, N.Y., 1974.
(9) E. Helfand, *Macromolecules*, **8**, 552 (1975).
(10) E. Helfand and Y. Tagami, *J. Chem. Phys.*, **56**, 3592 (1972).
(11) T. Inoue, T. Soen, T. Hashimoto, and H. Kawai, *J. Polym. Sci., Part A-2*, **17**, 1283 (1969).
(12) E. Helfand, *J. Chem. Phys.*, **62**, 999 (1975).
(13) See, for example, A. Guinier and G. Fournet, "Small-angle Scattering of X-rays", Wiley, New York, N.Y., 1955.
(14) G. Porod, *Kolloid Z. Z. Polym.*, **124(2)**, 83 (1951); **125(1)**, 51 (1952); **125(2)**, 108 (1952).
(15) P. Debye, H. R. Anderson, Jr., and H. Brumberger, *J. Appl. Phys.*, **28**, 679 (1957).
(16) C. G. Vonk, *J. Appl. Crystallogr.*, **6**, 81 (1973).
(17) D. F. Leary and M. C. Williams, *J. Polym. Sci., Part B*, **8**, 335 (1970); *J. Polym. Sci., Polym. Phys, Ed.*, **11**, 345 (1973).
(18) E. Helfand and A. M. Sapse, *J. Chem. Phys.*, **62**, 1327 (1975).
(19) E. Helfand, *Acc. Chem. Res.*, **8**, 295 (1975).
(20) E. Helfand and Z. R. Wasserman, to be published in *Macromolecules*.
(21) D. J. Meier, private communication.
(22) E. Helfand, private communication.
(23) A. Todo, M. Fujimura, T. Hashimoto, and H. Kawai, to be published.
(24) The effect of truncating the higher order terms has been recently examined by Hashimoto et al.[23] The results indicate that inclusion of higher order terms yields greater values for σ and t.
(25) It is noted that the first maximum of amorphous scattering of polystyrene is located at the Bragg angle (2θ) 9.8°, while the maximum of polyisoprene is at ca. 14°.
(26) It should be noted that the restriction of the symmetric block has been removed in the recent calculations of Meier.[21]
(27) It is pointed out by Helfand[22] that the Debye length t_D should be divided by a factor of $3^{1/2}$ when it is compared with the interphase thickness. This is because the interphase width is in one direction only, while the Debye length refers to an isotropic phenomenon.

Magic-Angle ^{13}C NMR Analysis of Motion in Solid Glassy Polymers

Jacob Schaefer,* E. O. Stejskal, and R. Buchdahl

Monsanto Company, Corporate Research Department, St. Louis, Missouri 63166.

Received June 14, 1976

ABSTRACT: The dipolar-decoupled, natural abundance Fourier transform and cross-polarization ^{13}C NMR spectra of seven glassy polymers have been obtained at 22.6 MHz, both with and without 3-kHz mechanical spinning at the magic angle. The 100-Hz resolution achieved by the spinning produces spectra of the solids almost as detailed as the standard spectra of the same polymers in solution. This kind of resolution allows individual lines to be assigned to chemically unique carbons both in the side and main chains of the polymers. Spin–lattice, nuclear-Overhauser, rotating-frame, and cross-polarization relaxation parameters have been measured for individual carbon lines at room temperature. The ^{13}C rotating frame relaxation times ($T_{1\rho}$) at 32 kHz can be shown to be dominated by spin–lattice processes rather than spin–spin processes. This means that the $T_{1\rho}$'s contain information about the motions of the polymers in the 10–50 kHz region, while the cross-polarization relaxation times (T_{CH}) contain information about the near static interactions. The spin–lattice and nuclear-Overhauser relaxation parameters contain information about the motions in the 5–30-MHz regions. Interpretation of the $T_{1\rho}$'s of these polymers emphasizes the dynamic heterogeneity of the glassy state. Details of the relaxation processes establish the short-range nature of certain low-frequency side-group motions, while clearly defining the long-range cooperative nature of some of the main-chain motions, the latter not consistent with a local-mode interpretation of motion. These motions involve cooperative torsional oscillations within conformations rather than jumps from one conformation to another. The ratio of T_{CH} to $T_{1\rho}$ for protonated carbons in the main chain of each polymer is found to have a direct correlation with the toughness or impact strength for all seven polymers. This empirical correlation is rationalized in terms of energy dissipation for chains in the amorphous state in which low-frequency cooperative motions (and ultimately flow) are determined by the same inter- and intra-chain steric interactions which influence the NMR relaxation parameters.

I. Introduction

We have three objectives in this paper. First, we will show that the rotating-frame ^{13}C relaxation parameters obtained from high-resolution ^{13}C NMR spectra of glassy polymers can be interpreted unambiguously in terms of the side- and main-chain motions of the polymers in the solid state (sections IV–VI). Second, we will show that an understanding of the